7ICMSNSE-103

### On CFD Methodology for Simulations of Whole Reactor Flow

# **Xue-Nong Chen**<sup>1</sup>

<sup>1</sup> Karlsruhe Institute of Technology, Karlsruhe, Germany xue-nong.chen@kit.edu

#### **Abstract**

This paper deals with the method how to apply a CFD code for whole reactor core and vessel flow simulations and overviews the recent developments in this topic. Two methods are introduced, namely coupling a channel model with CFD via boundary conditions and embedding a macroscopic channel model in CFD via differential equations. The latter one is recommended and further discussed in this paper, because there is a significant difficulty in realization of the former one. For treating heterogeneous core structure of pin bundle and wrapper, models of macroscopic pin bundle and fuel pin temperature are introduced and discussed. Numerical results based on SIMMER-III code are presented for a steady state as a subchannel benchmark in a LBE cooled reactor and for a power excursion in sodium cooled fast reactor. It is concluded that CFD with the embedded channel model can simulate the whole reactor flow without loss of details of subchannel characteristics.

**Keywords:** Reactor Thermal Hydraulics, CFD, Macroscopic Subchannel Model, Pin Bundle Flow

#### 1. Introduction

The traditional method that was successfully applied and widely performed for nuclear reactor safety analyses is based on the 1-D or 1-D plus channel method. However, there are many multidimensional thermal-hydraulics phenomena cannot be neglected in the pool-type reactor, which is the main type for many advanced reactors. The multi-dimensional thermal-hydraulics phenomena in the pool-type reactor with important safety features includes for example the coolant mixing at the core upper plenum, the thermal stratification in the reactor vessel and natural convection in differently heated channels. Therefore, using 1-D system codes to conduct safety analyses of pool-type reactors is regarded as insufficient (IAEA, 2003) [1].

On the other hand, with rapid developments of the high performance computer technology and the computational fluid dynamics (CFD) method, multi-dimensional CFD simulations are available at present. The multi-dimensional CFD method has been widely used to solve multi-dimensional fluid dynamics problems in many industries, such as automotive and aircraft industries. The researchers of the new generation are in favour to apply CFD method to simulate multi-dimensional thermal-hydraulics phenomena in the reactor system. The advantages of the CFD method have been recognized by many research works, see e.g. Vanderhaegen et al., 2011; Chen et al., 2014, 2015, [2-4]. However, because of the limitation

of current computation capacity and the complex of the reactor core structure (pin bundle with wires and wrapper), a direct simulation of whole reactor flow with sufficiently fine meshes for the detailed pin bundle geometry is still not possible for a common routine reactor application. How to apply CFD method or code to simulate whole reactor flow with coarse meshes without loss of detailed sub-channel (SC) characteristics is the main question, which this paper deals with.

From the methodological point of view, two ideas based on "coarse meshes" of the channel size have been considered, where the pin bundle flow is still modelled by the channel method. One is to couple the channel method with the CFD one through boundary conditions. The other one is to imbed the channel model into the CFD one through differential equations based on the porous medium approach. The current author would like at first to point out difficulties in the former idea and then describe in details what one needs in the latter one. For treating heterogeneous core structure of pin bundle and wrapper, models of macroscopic pin bundle and fuel pin temperature are introduced and discussed. Numerical results based on SIMMER-III code are presented for a subchannel flow in a LBE cooled reactor [5] and a power excursion in sodium cooled fast reactor [6].

## 2. CFD-channel-model coupling methods

The whole reactor vessel can be divided into several regions, namely, core, upper and lower plena, bypass and primary heat exchanger and pump, as shown in Figure 1. The regions, which are filled 100% with coolant, e.g. the bypass, upper and lower plena, will be calculated of course directly by a CFD code. The other regions, which contain complicated solid structures of coolant channels, e.g. the core and the heat exchanger, will be simulated by a channel model. There are two methods to couple these two simulation models. One is to couple them via boundary conditions and the other via coefficients of differential governing equations.

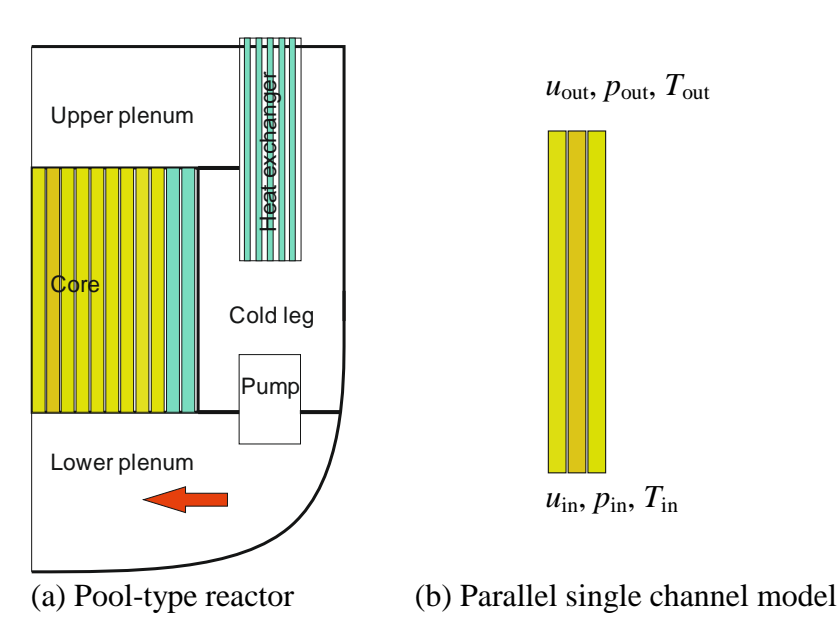


Figure 1 CFD simulation regions of a typical pool-type reactor

### 2.1 Matching channel model to CFD method via boundary conditions

This idea is quite natural, therefore many researchers think of it and try to realize it. In large coolant bulk regions, e.g. upper and lower plena and cold leg, as shown in Figure 1, are calculated directly by a CFD code. In the core region, as well as the heat exchanger one, because of the pin bundle structure, it is better to apply 1-D channel model or 1-D plus shubchannel model. To couple these two different codes, one has to match the regions by boundary conditions, whereby velocity, pressure and temperature are continuous, i.e. they are same on both sides of the boundary, for every time. This requirement seems to be simple, but difficult to be satisfied. We explain this difficulty with a simplified single channel model without taking account of temperature effect.

The circulation under the operation condition is in the clockwise direction, as shown by the red arrow in Figure 1 (a). This means for the reactor core, the flow is from the bottom to the top. For the sake of simplicity it is assumed that the coolant is incompressible. Thus, the mass flow rate is same everywhere in the channel. This means if  $v_{in}$  is known,  $v_{out}$  is also known. For the channel model, we should either give  $\Delta p = p_{\rm in} - p_{\rm out}$  as input and get  $v_{\rm in}$  and  $v_{\rm out}$  as output, or give  $v_{\rm in}$  and  $v_{\rm out}$  as input and get  $\Delta p$  as output, by solving the momentum equation. For the CFD model applied in other rest regions,  $p_{\text{out}}$  and  $v_{\text{out}}$  should be given as the inlet boundary conditions of the CFD region and p and v will be obtained as output at outlet boundary of the CFD region. But this obtained p and v are not necessarily the same as the  $p_{\rm in}$ and  $v_{\rm in}$ . Purely numerical iterations by changing channel model input, i.e. either the driving pressure or the flowrate, are needed. Although these iterations could be done by trial and error, it is quite difficult for a large number of parallel channels, where v and p are distributions over the core cross section. According to our own experiences with the Couple Code [7], it was even failed with this matching technique. Moreover, there is reverse flow locally in some cold open channels in some no-driving cases, e.g. natural convection case. This makes this matching/coupling more difficult. Therefore this is not the method that we recommend in this paper.

# 2.2 Embedding channel model in CFD method via coefficients of differential equations

There is another method, which can avoid above mentioned difficulty. This is based on the porous medium approach. In the following for the sake of simplicity we formulate this method only for the single phase flow. Considering now the pin-bundle structure as a kind of porous medium with fluid (coolant) volume fraction  $\alpha_c$ , the governing equations can be modified from those of fully fluid flow by replacing the fluid density  $\rho$  with the so-called macroscopic density (smear density)  $\bar{\rho} = \alpha_c \rho$ . Thus, the mass, momentum and energy conservation equations can be written formally as,

$$\frac{\partial \overline{\rho}}{\partial t} + \nabla \cdot (\overline{\rho} \mathbf{U}) = 0 \tag{1}$$

$$\frac{\partial \overline{\rho} u_i}{\partial t} + \nabla \cdot (\overline{\rho} u_i \mathbf{U}) = \alpha_c \left( -\frac{\partial p}{\partial x_i} + \rho g_i + S_i \right)$$
(2)

$$\frac{\partial(\overline{\rho}T)}{\partial t} + \nabla \cdot (\overline{\rho}\mathbf{U}T) = \alpha_c \left(\nabla \cdot \left(\frac{k}{c_p}\nabla T\right) + \frac{S_T}{c_p}\right)$$
(3)

where  $\mathbf{U} = (u_1, u_2, u_3)$  is the coolant velocity vector, T the coolant temperature,  $\mathbf{x} = (x_1, x_2, x_3)$  the coordinates and  $\mathbf{g} = (g_1, g_2, g_3)$  the gravity force. If  $x_3$  is the upward z-coordinate, then  $\mathbf{g} = (0, 0, -g)$ , where g is the acceleration due to gravity. The term  $S_i$  in Eq. (2) represents the momentum loss (or pressure loss) either due to the viscose dissipation in the interior flow or the viscose friction on solid structure boundaries, which will be discussed in detail. Eq. (3) is the thermal energy conservation one, which will be not dealt with in this paper, although the heat transfer process from the fuel to coolant is modelled in the pin thermal model [4], is not discussed here, especially for the external heat source term  $S_T$ . The pump effect can be modelled by adding a delta function at the certain position with the amplitude of pump head to the pressure gradient term.

Before we treat the momentum loss term especially for the pin-bundle structure in the core, let's first consider it for the 100% coolant filled regions. Obviously it should stay in its original form of Navier-Stockes equations as,

$$S_i = \nabla \cdot \left(\mu \nabla u_i\right) \tag{4}$$

where  $\mu$  is the coolant viscosity. However, from the pressure loss point of view this term can be neglected, since it contributes relatively very small pressure loss in the large coolant bulk regions compared to narrow channels in the core and heat exchanger regions, although it is responsible for complex fine turbulent flow structures. Another reason for neglecting this term is that the meshes are too coarse to calculate this term. Indeed the momentum equation in those regions becomes Euler type.

The reactor core will be modelled by a channel model. The simplest channel model is the single channel one, where a whole sub-assembly (SA) is modelled as an average channel, which has no heat exchange with other surrounding channels. The momentum loss term in the axial direction (i = 3) is actually the pressure drop correlation and expressed as

$$S_i = \frac{1}{2} \rho |u_i| u_i \frac{C_f}{D_H} \tag{5}$$

where  $\mu$  is the coolant viscosity,  $D_H$  the equivalent hydraulic diameter and  $C_f$  the pressure drop coefficient. The most famous and widely applied pressure drop correlations are the Hagen-Poiseuille for the laminar flow and the Blasius for the turbulent flow, expressed as

$$C_{f} = \begin{cases} \frac{64}{Re_{D_{H}}} & \text{for } Re_{D_{H}} \leq Re_{0} \\ \frac{0.3164}{Re_{D_{H}}^{0.25}} & \text{for } Re_{D_{H}} > Re_{0} \end{cases}$$
 (6a)

with

$$D_H = \frac{4A}{L_{...}}, Re_{D_H} = \frac{\rho |u_i| D_H}{\mu}, Re_0 \approx 1187$$
 (6b)

where A is the flow cross-section area and  $L_w$  the wetted perimeter of the cross section.  $Re_0$  is the critical value of the Reynolds number, which is roughly the cross point of the two curves in (6a).

Now we can summary the momentum conservation law (2) in different regions with a unified equation as,

$$\frac{\partial \overline{\rho} u_i}{\partial t} + \nabla \cdot (\overline{\rho} u_i \mathbf{U}) = \alpha_c \left( -\frac{\partial p}{\partial x_i} + \rho g_i + \frac{1}{2} \rho |u_i| u_i \frac{C_f}{D_H} \right)$$
(7)

where in the large coolant bulk regions  $C_f$  is zero and in the channel regions  $C_f$  is given as in (6). In addition in the channel region the lateral velocities disappear, i.e.  $u_1 = u_2 = 0$ , only  $u_3$  remains. It is to be reminded that the coolant volume fraction  $\alpha_c$  is also a function of space.

Obviously this method can be easily implemented in any CFD code without changing numerical scheme and without any iteration, i.e. its calculations can be performed without any difficulty. This is known to many experienced researchers, e.g. see [2-4]. What is not so well-known is that the channel model can be improved, so that the sub-channel flow can be characterized as well with this CFD method [5]. In the following section the subchannel flow modelling will be reviewed.

### 3. Macroscopic pin bundle model for the CFD method

The channel model scale (mesh size) can be based on sub-assembly (SA) and also on sub-channel (SC). The former one is very coarse, which only provides results in the sense of SA average. If one wants to have more detailed information, one should consider finer meshes, the latter one. Actually it is necessary to consider the subchannel scale, while the flows in the side/corner channels and the interior ones are significantly different. This difference has not only significant impacts on the steady state (velocity and temperature distributions in an SA), but also on transients, as we will show in our examples. The macroscopic pin bundle model for CFD application has been already developed in [5]. The basic idea of this model is to distinguish the side channels and the interior channels and to include cross flow effect by taking account of the local pressure drops in every direction, since it is dominant and the

pressure drop due to momentum exchange between channels is relatively weak. In the following it will be reviewed briefly.

# 3.1 Geometrical arrangement

As well-known there are three types of subchannels, namely interior, side, and corner ones. For the pin bundle configuration with wire spacer, the side channels have double flow area of the interior one and but the same power as the interior one, as both types of channel have a half associated fuel pin. Moreover the hydraulic diameter of the side channel is larger than the interior one by roughly 20%. The characteristics of these two types of subchannels is shown in Fig. 2. The number of corner channels is always equal to 6 and usually relatively small compared to those of other two types of subchannels, nevertheless they have similar characteristics to side channels, i.e. less power density and larger hydraulic diameter than the interior one.

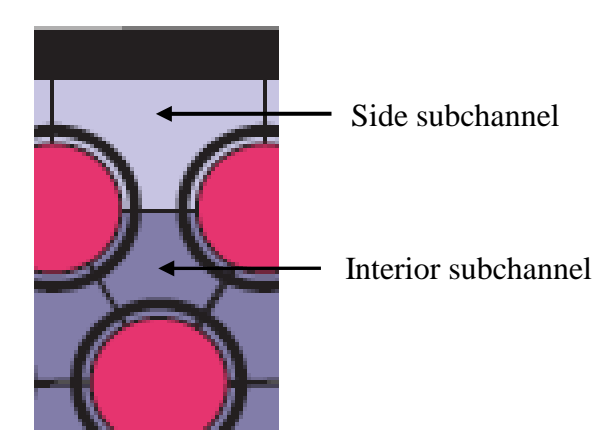


Figure 2 Side subchannel vs. interior subchannel

Geometrically the side/corner and interior subchannels should be lumped separately. In 2-D cylindrically symmetric case for example, the central fuel SA can be arranged as illustrated in Figure 3 for a LBE cooled reactor [5] and the off-central fuel SAs in Figure 4 for sodium cooled reactor [6].

The most important geometrical parameters are the coolant volume fraction  $\alpha_c$  and the wetted structure surface area per cell volume  $a_s$ . Indeed, the hydraulic diameter  $D_H$  can expressed as

$$D_H = \frac{4\alpha_c}{a_c} \tag{8}$$

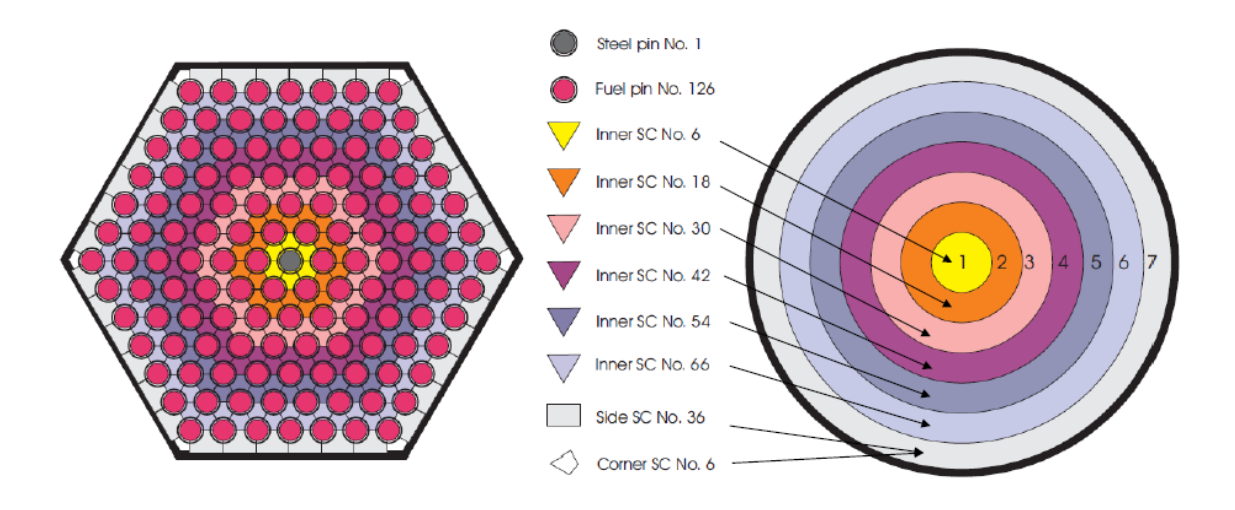


Figure 3 The central fuel assembly and its ringwise subchannel arrangement in the case of [5]

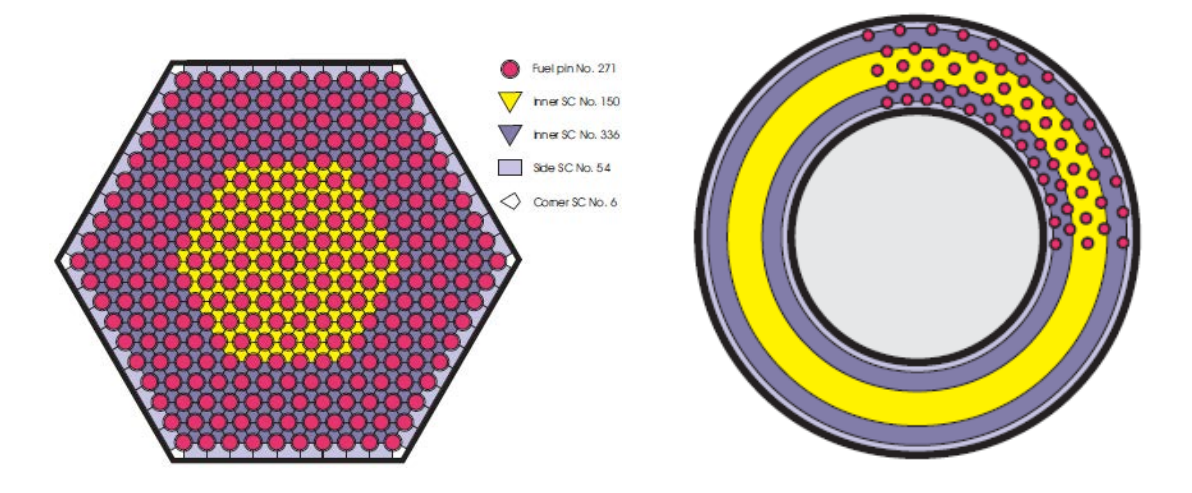


Figure 4 Fuel assembly is divided into three sub-regions (left plot), which are transformed to five sub-rings in one original SA ring (right plot) in the case of [6]

# 3.2 Frictional drags and pressure drops

For the sake of simplicity, we now discuss only the 2-D cylindrical symmetric case, where the radial and axial velocities are denoted as u and v. Because of the heterogeneous pin-bundle structure, the pressure drops are anisotropic. Both the radial and the axial pressure drops are related to the frictional drags, which are experienced by the pins and wrappers. Conventionally, the axial and radial drag coefficients are defined as

$$C_{D,radial} = \frac{f_D}{\frac{1}{2}\rho u^2 d}, \ C_{D,axial} = \frac{\tau_w}{\frac{1}{2}\rho v^2}$$
 (9)

where  $f_D$  is the viscous drag per unit pin length in the radial direction,  $\tau_w$  the viscous drag shear stress on the pin and wrapper surface in the axial direction and d the pin outer diameter. We assume that the pressure drop in each direction is independent from the flow in other directions. Therefore we can write the momentum exchange terms in (2) as

$$\alpha_c S_r = -K_r u \,, \qquad \alpha_c S_z = -K_z v \tag{10}$$

By the momentum balance in a macroscopic control volume, we can derive the pressure drop in the radial and axial directions in terms of the drag coefficients as

$$K_r = C_{D,radial} \frac{1}{2} \rho |u| \frac{4(1 - \alpha_c)}{\pi d} \tag{11}$$

$$K_z = \frac{\alpha_c}{2D_H} C_f \rho |v| \quad \text{with } C_f = 4C_{d,radial}$$
 (12)

The axial flow is usually dominant and there are various correlations for  $C_f$ . One of them is (6a), which holds also in this case. In contrast the radial flow (in general the cross flow) is usually quite small and there are not so many correlations, especially for the pin bundle cross flow. We may apply the correlation suggested by Tanino and Nepf [8] for the cross flow over a cylinder array, repeated here as

$$C_{D.radial} = 2\left(\frac{a_0}{Re_d} + a_1\right) \text{ with } a_0 = 84 \text{ and } a_1 = 0.46 + 3.8(1 - \alpha_c)$$
 (13)

where  $Re_d$  is defined based on the radial flow velocity u and the pin diameter d as

$$Re_d = \frac{\rho|u|d}{\mu} \tag{14}$$

So far we have completed the macroscopic pin bundle momentum exchange model. The model has been implemented in the SIMMER code [9, 10] and two calculation examples will be shown in the next section.

It should be mentioned that the momentum exchange effect between subchannels due to their different axial velocities and its enhancement by the wires are not discussed in this paper. These should be further studied and the corresponding model should be developed.

## 4. Numerical examples

### 4.1 Lead-bismuth-eutectic cooled MYRRHA critical reactor

As the first numerical calculation example we consider the lead-bismuth-eutectic (LBE) liquid cooled MYRRHA critical core design (critical mode of FASTEF) [11]. The SIMMERIII thermal hydraulic and neutronic coupled calculation model of this design was set-up within the project of Central Design Team (CDT). Although the SIMMER model deals with whole core simulation, we concentrate here, by presenting the model and its results, on a single subassembly in order to emphasize pin bundle (subchannel) effects. The central in-pile-section (IPS) assembly in the original design was replaced by a fuel assembly (FA) for the current simulation and apply the pin-bundle model to this central fuel assembly [5]. The geometrical parameters of FA and fuel pin and their arrangements can be found in [11]. The central fuel assembly is divided into 7 rings, as already shown in Figure 3. In the steady state benchmark calculation, the central pin is a steel pin. Therefore the power distribution has a depression at the centre.

For the steady state benchmark calculation we choose the example calculated by the Subchanflow code [5, 11] in the framework of the CDT project [11]. The outlet coolant velocity and temperature calculated by the both codes are compared in Figure 5. The difference in the average outlet temperature is due to different values of LBE heat capacity used in the codes. Both temperature and velocity results of the two codes agree well. The axial and radial velocity distributions in this fuel assembly are shown in Fig. 5. In the fuel assembly centre the axial velocity is lowest, because there is no power in the central steel pin. In the peripheral ring (Ring 7) the axial velocity is highest, because the hydraulic diameter is largest there. The radial velocity in the steady state is quite small, as reported in [5]. Its maximal Reynolds number is about 40.

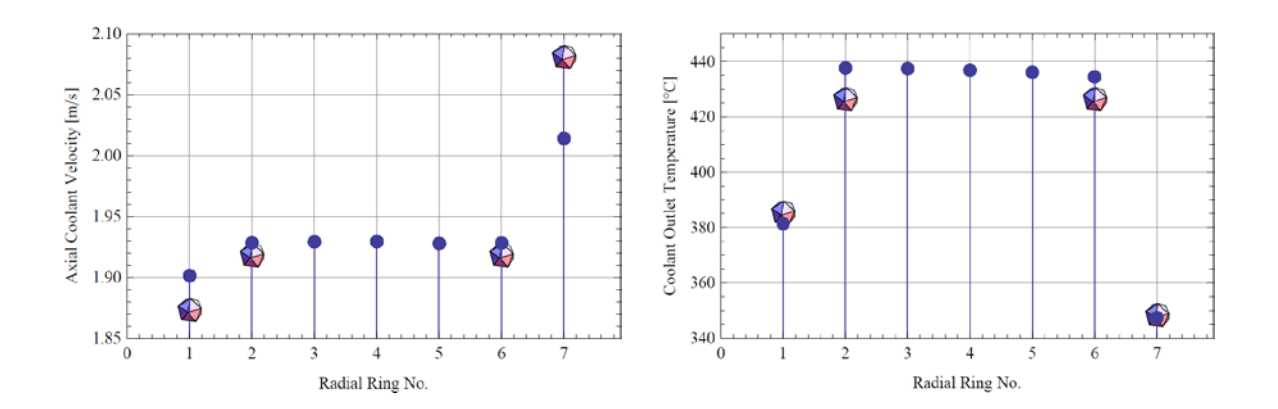
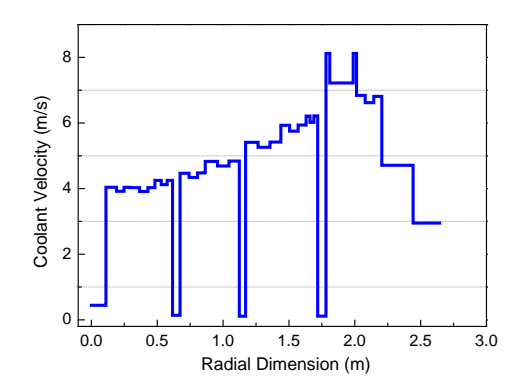


Figure 5 Axial outlet coolant velocity distribution (left plot) and outlet coolant temperature distribution (right plot), where the points stand for the current SIMMER results with the pinbundle model and the marks for the Subchanflow ones [5, 11].

### 4.2 European Sodium Cooled Fast Reactor (ESFR)

The second numerical example we take is the unprotected loss of flow (ULOF) in ESFR [6]. In this case the sodium boiling takes place. Because of its positive void worth, this sodium boiling triggers a power excursion. It was recognized that the SA scale single channel model (denoted as "coarse meshes" in this example), overestimates the reactivity insertion ramp artificially, since the sodium boiling takes place simultaneously in a whole SA ring. The SC scale channel model (denoted as "fine meshes" in this example) can retard this process significantly because it distinguishes the difference of velocity and temperature in the side and interior subchannels [6].

The hottest fuel assembly ring is divided into 5 subrings in the fine mesh modelling, as already shown in Figure 4. The steady state results of the fine mesh simulation are presented in Fig. 6. It is clearly seen, in particular from the hottest SA rings at about r=2 m, that the coolant velocity in the side subchannel is higher than that in the interior one, while the coolant outlet temperature in the side subchannel is significantly lower than that in the interior one. The temperature difference between them is 100 K in the hottest fuel SA ring, while the velocity difference there is 0.9 m/s. As mentioned before this temperature difference leads to a significant retardation of reactivity insertion due to the coolant boiling in the ULOF transient. Since we want to compare the fine mesh results with the coarse mesh one, we give here some typical values for the hottest SA in the steady state. The coolant outlet velocity and temperature are 7.33 m/s and 817 K in the coarse mesh calculation, while the minimal and maximal coolant outlet velocities are 7.22 m/s and 8.12 m/s and the minimal and maximal coolant outlet temperatures are 740 and 840 K in the fine mesh calculation.



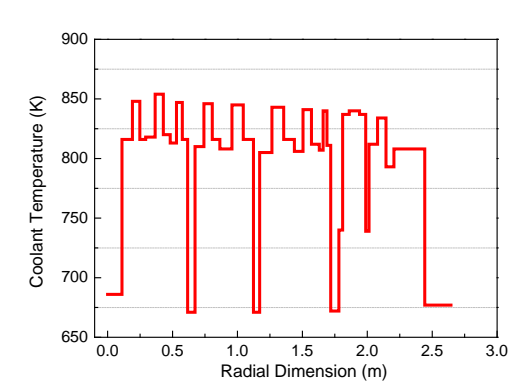
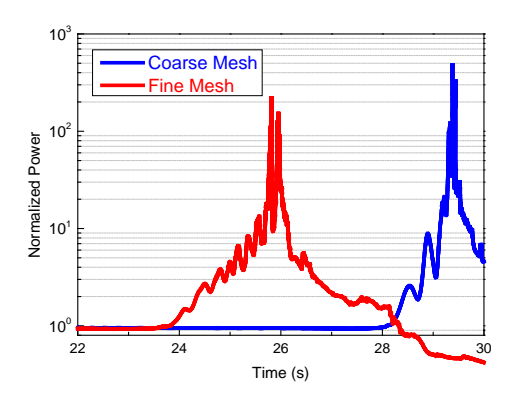


Figure 6 Radial coolant outlet velocity (left) and temperature (right) distributions [6]

ULOF results of fine mesh simulation are presented together with those of the coarse mesh. The power and reactivity transients are plotted in Fig. 7. The boiling on-set takes place earlier in the fine mesh simulation (at about t = 23 s after the ULOF start) than in the coarse one (at t = 27.0 s), because the hottest coolant temperature is higher in the fine mesh simulation than the average SA coolant temperature in the coarse one. Therefore the first power excursion is triggered earlier in the fine mesh calculation. After the boiling onset, the reactivity and power

transients have more and smaller oscillations in the fine mesh simulation than in the coarse one. The power excursion is broader in the fine mesh simulation than in the coarse one. The power excursion is delayed for almost 1 second counted from the sodium boiling onset by the fine mesh simulation. As a consequence, the power peak is significantly reduced and the reactivity insertion is retarded from the sodium boiling onset by the fine mesh simulation. The highest power amplitude is reduced from 480 times in the coarse mesh case to 220 times in the fine mesh case, as shown in Fig. 7. However, the thermal energy release by the power excursion is roughly the same in both simulations, as the power is integrated over the period.



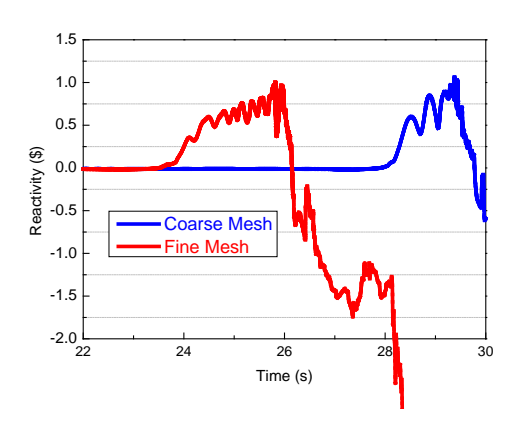


Figure 7 Power (left) and reactivity (right) histories calculated by coarse meshes in the size of SA (blue) and fine meshes in the size of SC (red)

#### 5. Conclusion

It has been reviewed that the channel models can be embedded in the CFD method or code, so that the whole reactor flow can be simulated without losing any detailed characteristics of the core subchannel flow. The macroscopic pin-bundle model plays an important role here. The numerical results show that (i) the macroscopic pin-bundle model can predict similar results as the subchannel code; (ii) the mesh size has significant impact on the power excursion transient.

### 6. Acknowledgements

The author appreciates the effort and support of all the scientists and institutions involved in MAXSIMA, as well as financial supports of the European Commission through the contract FP7-323312. Especially the author thanks his colleague Dr. V. Kriventsev for his comment on improvements of the macroscopic pin bundle model.

#### 7. References

[1] IAEA, "Use of computational fluid dynamics codes for safety analysis of nuclear reactor systems", IAEA-TECDOC-1379, 2003.

- [2] M. Vanderhaegen, J. Vierendeels, B. Arien, "CFD analysis of the MYRRHA primary cooling system", Nuclear Engineering and Design, Vol. 241, 2011, pp. 775-784.
- [3] Z. Chen, P. Zhao, G. Zhou and H. Chen, "Study of core flow distribution for small modular natural circulation lead or lead-alloy cooled fast reactors", Annals of Nuclear Energy, Vol. 72, 2014, pp. 76-83.
- [4] Z. Chen, X.-N. Chen, A. Rineiski, P. Zhao and H. Chen, "Coupling a CFD code with neutron kinetics and pin thermal models for nuclear reactor safety analyses", Annals of Nuclear Energy, Vol. 83, 2015, pp. 41-49.
- [5] X.-N. Chen, R. Li, A. Rineiski and W. Jäger, "Macroscopic pin bundle model and its blockage simulations", Energy Conversion and Management, Vol. 91, 2015, pp. 93-100.
- [6] X.-N. Chen, A. Rineiski, F. Gabrielli, L. Andriolo, B. Vezzoni, R. Li and W. Maschek, "Fuel-steel mixing and radial mesh Effects in power excursion simulations", Submitted to Annals of Nuclear Energy, 2015.
- [7] D. Zhang, Z.-G. Zhai, X.-N. Chen, S. Wang and A. Rineiski, "COUPLE, a coupled neutronics and thermal-hydraulics code for transient analyses of molten salt reactors", Transactions of American Nuclear Society Annual Meeting, Atlanta, USA, 2013.
- [8] Y. Tanino and H.M. Nepf, "Laboratory investigation of mean drag in a random array of rigid, emergent cylinders", J. Hydraulic Engineering, Vol. 134, 2008, pp.34-41.
- [9] Sa. Kondo, Y. Tobita, K. Morita and N. Shirakawa, "SIMMER-III: an advanced computer program for LMFBR severe accident analysis", <u>Proc. International Conference on Design and Safety of Advanced Nuclear Power Plant (ANP'92)</u>, Vol. IV, Tokyo, Japan, pp. 40.5.1–40.5.11, 1992.
- [10] Sa. Kondo, Y. Tobita, K. Morita, et al., "Current status and validation of the SIMMER-III LMFR safety analysis code", <u>Proc. 7th International Conference on Nuclear Engineering (ICONE-7)</u>, Paper No. 7249, Kyoto, Japan, 1999.
- [11] M. Sarotto, D. Castelliti, R. Fernandez, D. Lamberts, E. Malambu, A. Stankovskiy, W. Jaeger, M. Ottolini, F. Martin-Fuertes, L. Sabathé, L. Mansani and P. Baeten, "The MYRRHA-FASTEF cores design for critical and sub-critical operational modes (EU FP7 Central Design Team project)", Nuclear Engineering and Design, Vol. 265, 2013, pp. 184-200.

 $7^{th}$  International Conference on Modelling and Simulation in Nuclear Science and Engineering (7ICMSNSE) Ottawa Marriott Hotel, Ottawa, Ontario, Canada, October 18-21, 2015